Subtractive Shading Envelope's Computational Workflow

Subjects: Energy & Fuels
Contributor: Miktha Alkadri

This study proposes a voxel-based design approach based on the subtractive mechanism of shading envelopes and attributes information of point cloud data in tropical climates. In particular, the proposed method evaluates a volumetric sample of new buildings based on predefined shading performance criteria. With the support of geometric and radiometric information stored in point cloud such as position (XYZ), color (RGB), and reflection intensity (I), an integrated computational workflow between passive design strategy and 3D scanning technology is developed. It aims not only to compensate for some pertinent aspects of the current 3D site modelling such as vegetation and surrounding buildings but also to investigate surface characteristics of existing contexts such as visible sun vectors and material properties. These aspects are relevant for conducting a comprehensively environmental simulation while averting negative microclimatic impacts when locating the new building into the existing context. Ultimately, this study may support architects for taking decision-making in conceptual design stage based on the real contextual conditions.

Keywords: voxel-design approach ; shading envelopes ; point cloud data ; computational design method ; passive design strategy

---

1. General Background

The rapid development of 3D laser scanning technology has reached across multiple-disciplines within design and engineering. However, the practical implementation of this technology is often applied in major fields, such as photogrammetry [1][2], cultural heritage [3][4][5][6], and environmental engineering [7][8]. Digital reconstruction as one of the main subjects in these scopes has been used predominantly for building performance assessments [9][10], where the contextual modeling of existing studies is frequently based on a 3D solid modeling context [11][12]. As a consequence, high computational costs and time are required to cover the entire set of complex building forms. On the other hand, the use of point clouds during the early stage of architectural design has not yet been fully explored, especially related to the performance simulation task and design decision support.

As an entity of 3D data scanning, Otepka et al. [13] illustrate the point cloud as a universal denominator for laser scanning and photogrammetric data. Its data structure is principally characterized by position information (XYZ) as a permanent element coupled with auxiliary information attached to it, such as color attributes (RGB), reflection intensity (I), and any abstract information [14]. The prospective applications of these attributes not only represent metadata information of the real environment, but also enable designers and researchers to perform numerous tasks, such as data processing, visualization, and analysis. Moreover, this can help architects further to address environmental design issues, such as solar and shading performance.

The technological advancement of point cloud reveals the relevance of integrating it into the passive design strategy, especially when dealing with generative architecture designs that currently lack several relevant aspects. For example, first, understanding the site characteristics of an existing environment. While 3D site modeling primarily deals with a building-oriented context, surrounding properties, such as vegetation and adjacent buildings, are often neglected [15]. This may not only affect the performance simulation of a proposed design, but also potentially create microclimatic issues when it comes to the real context. Second, the absence of surface properties, such as roughness and material characteristics on a manually-built 3D model, may cause a crucial discrepancy when dealing with environmental simulation between planned and existing buildings [16]. With geometric and radiometric information extracted from point cloud data, this study, therefore, proposes an integrated passive design approach based on shading performances of new and existing contexts.

As a contextual design approach, this study specifically investigates the idea of subtractive shading envelopes that are principally extracted from the concept of solar envelopes initially introduced by Knowles [17]. In this regards, solar envelopes permit architects to design appropriate massing of a new building into the existing environment by guaranteeing desirable sun access for surrounding buildings during the critical period [18], while subtractive shading approach aims to extract potential performances of the existing contexts and integrate it with a 3D volumetric massing of a proposed building based on predefined shading performance criteria.

Since then, various computational methods of solar envelopes, such as descriptive geometry, solar obstruction angle, and constructive solid geometry have been defined [19]. These approaches have successfully demonstrated the concept of solar envelopes into various urban settings (e.g., single building, open space, and urban scale) and multiple functional utilities (e.g., housing, offices, and commercial buildings). It is worth noting that the contextual settings of the existing methods primarily focus on temperate zones of southern and northern hemisphere countries, which have distinct climatic conditions during the four-seasons. This means that design objectives and climatic parameters of most existing methods for solar envelopes become less applicable when it comes to tropical countries, especially for those located on the Equator, such as Indonesia. Since tropical countries present wet and dry seasons all year round, the objective of solar envelopes significantly shifts and aims to minimize the penetration of direct sun access to the buildings, due to high temperatures. For example, housing in Indonesia is typically designed in a way that prohibits direct sunlight from penetrating the dwelling, especially into primary living spaces, so that temperatures are kept low during the day. Consequently, the air conditioner (AC) frequently becomes a short-term solution to mitigate the building’s temperature, which unfortunately contributes to the annual increase in energy consumption [20]. Accordingly, shading conditions become considerably relevant for urban forms generation in tropical contexts. This study specifically proposes an environmental design strategy that integrates shading performance aspects and attributes information from point cloud data through a computational workflow of a voxel-based design approach.

2. Related Works

2.1. Solar Envelopes

In the remote past, the concept of vernacular architecture has successfully contributed to preserving sustainable building envelopes [21][22]. This can be observed through the development of the Indus Valley, Mohenjo-Daro in India, 2500 BC [23], El-Lahun village in Egypt (1857–1700 BC) [24], and many classical Greek cities, such as Olynthus in North Hill—a city designed to benefit from passive solar energy for the heating of buildings [25]. This strategy was known as solar-oriented homes or so-called “solar architecture”. Since then, solar architecture has become an essential guide for designers to develop sustainable urban planning. For example, Andrea Palladio has discussed the proper norms of city planning by considering wide streets for cold climate countries and narrow streets for tropical countries [26]. Additionally, Ildefons Cerdà integrated green areas into the public and private space of Barcelona in his masterplan of the city so as to enhance the comfort of inhabitants [27]. During the industrial revolution, the idea of urban solar policy or refers to the post-war housing was also implemented in France (in 1912), Germany (in 1920), and New York (in 1916). These examples have shown a positive contribution to architectural buildings, not only to reduce the energy consumption of the built environment [28], but more importantly, to support a healthy living environment [29]. Furthermore, the idea of solar accessibility has been elaborated further through the concept of solar envelopes.

By definition, solar envelopes stand for imaginary boundaries that are constructed based on the sun’s movement. It is regulated based on specific space-time constraints [18]. According to this principle, solar envelopes can be transformed into geographic and climatic properties within the size of on-site buildings [19]. Geographic properties deal with a group of parameters that define the spatial relationship between the design plot and existing context related to orientation typology, surrounding facades, sidewalks, building height, longitude, latitude, floor area ratio (FAR), setback, shadow fences, and street sizes. On the other hand, climatic properties consist of parameters that determine the geometric transformation of the proposed building based on the time construction, such as cut-off-times, solar angle, sun path, dry bulb temperature, sun access hours, solar altitude, and solar azimuth. These parameters are used not only to generate solar envelopes but also to identify the character and qualities of the built environment. For example, orientation plays a great role in examining the geometrical shape of solar envelopes, especially when dealing with the street layout in relation to various angular values, colonnades with a variety of direct solar radiations, and solar urban layouts [30]. A seasonal leaf cover from the surrounding vegetation can also affect the geometrical configuration of solar envelopes as it may be considered as a part of geographic elements for violating excessive direct sun access during summer [16]. Besides, the solar angle as a climatic property is used to determine geometric solar envelopes based on the construction planes [31]. It is mostly employed for simple shape plots, with borders aligned with the main cardinal directions in east-west (EW) and north-south (NS) and for the main hours and days, such as the noontime during summer and winter solstice, and spring/autumn equinoxes.

2.2. Shading Envelopes

As opposed to solar envelopes, the concept of shading envelopes primarily deals with the solar radiation-reduction to achieve appropriate daylight for urban equatorial climates. This permits architects not only to establish a geometrical configuration of solar shading envelopes but also to control the direct sun exposure of the building's own façades and surroundings during a critical time. Two different types of shading approaches are identified as follows:

- Building forms

  In this part, the concept of shading envelopes aims to promote a passive design strategy through the form generation within the conceptual design stage. This means that the volumetric shape of proposed buildings is developed based on the consideration of solar shading criteria. An interesting example can be observed through the concept of "shadow umbrella" introduced by Emmanuel [32]. This concept proposed a design approach of shading strategies incorporated with natural elements, such as vegetation and water bodies, aiming to create shading for adjacent buildings and to mitigate the urban heat island for tropical neighborhood areas. Accordingly, a new configuration of urban block shapes with a thermally comfortable can be generated. DeKay [33] addressed a similar strategy with the concept of climatic envelopes. The climatic envelope primarily aims to generate a building mass that guarantees access for diffused daylight and solar energy resources for the surrounding buildings. This concept specifically contains a geometrical intersection between daylight and solar envelopes based on the sky exposure plane and solar protection plane, respectively. In this case, sky exposure plane refers to imaginary sloping planes that allow penetration of natural light and air on the building facades in higher density districts [34]; meanwhile, solar protection plane refers to an inclined plane that is generated from the profile angle, the so-called vertical shadow angle (VSA) [35]. In a similar vein, Capeluto [36] proposed the concept of self-shading envelopes by extending the functional properties of the sky exposure plane through the solar collection envelopes (SCE) model. The geometrical configuration of self-shading envelopes results in cone shapes, due to the required façade inclination and shading orientation. Therefore, the envelope's roof areas should be larger than the bottom part of the envelope geometries. This approach aims to avoid overheating and at the same time, to maximize the self-building protection for a certain period during summer.

- Building components

  In addition to building forms, shading approaches are also applied to specific building components, such as windows, cantilevers, and openings on the building façade, based on the determined building shapes. Although this study limits the scope of investigation on a form-finding design solution, some studies on shading mechanisms drive potential efforts to handle more complex projects. For example, Yezioro and Shaviv [37] proposed SHADING as a design and evaluation tool for analyzing mutual shading between buildings and other surrounding properties, such as vegetation. It specifically calculates the insolated fraction on the building surfaces quantitatively and performs a ray-tracing algorithm to identify the shadows visually at a particular time. Similarly, Marsh [38] also used a ray-tracing analysis to identify the external obstruction of solar intensity on the optimized shape of shading geometries. In this case, optimized shading designs have effectively accommodated passive solar control through the building apertures [39][40] Other approaches deal with a graphic solution of shading design tools [41], form-finding of static exterior shading devices called SHADERADE [42], and a cellular method to define optimal shading patterns [43].

Although these approaches may address the aspect of tropical design contexts, they lack some critical aspects during the simulation of shading envelopes. First, the quality of solar radiation (i.e., the quantity of direct sunlight hours) received by surrounding buildings is not taken into account by most methods and tools, due to a fixed period when determining direct sun access. Consequently, all geometrical shapes of existing buildings are treated similarly when receiving the irradiation qualities without considering the obstruction of properties and building orientation of the plot. Second, shadow fences of surrounding buildings' facades are primarily regulated by a Z-axis. This makes the design configuration of the resulting envelopes rely only on the horizontal shading lines. In fact, shading areas of surrounding façades are more complex, especially when dealing with dense areas and multiple urban forms. In order to compensate for these issues, the existing studies present some relevant aspects, such as subtractive mechanism and point cloud data that may be useful for further development. This will be discussed in the following section.

2.3. Subtractive Solar Envelopes

As previously mentioned in the general background, this approach specifically subtracts a volumetric matrix of the 3D plot according to solar accessibility criteria. This is done by projecting solar vectors acquired from the number of direct sunlight hours on surrounding building facades. In principle, this mechanism has been addressed by Leide and Schlüter [44][45] via volumetric site analysis (VSA). Their approaches aim to explore urban site information by simulating multiple environmental performances, such as solar radiation, airflow, visibility, thermal comfort, and wind velocity through volumetric insolation analysis (VIA), volumetric visibility analysis (VVA), and computational fluid dynamics (CFD). Such this approach and other related developments [46][47][48], however, merely focus on the architectural form-finding without any further consideration on the concept and design principles of solar or shading envelopes.

On the other hand, De Luca [49][50][51] and Darmon [52] have proposed a similar subtractive mechanism based on the performance criteria of solar envelopes or so-called subtractive solar envelopes. This approach specifically involves sun visibility that aims to evaluate sun vectors from a predefined shadow grid of surrounding building windows without any obstruction from other existing buildings. In parallel, ray-tracing analysis is performed from surrounding windows to the voxels within the 3D plot using a Boolean expression (true or false statement). In this operation, the true statement will be executed when sun vectors hit or intersect the 3D polyhedra, and accordingly, the voxels subtraction procedure to the 3D polyhedra can be performed. Meanwhile, the false statement indicates an unsuccessful intersection. This condition means that voxels that are not intersected may contribute to the generation of geometric solar envelopes.

The subtractive solar envelopes ultimately permit architects not only to deal with various geometric configurations based on solar performance analysis, but also to highlight the potential use of voxel-based generative designs for urban environments. However, despite such potential improvements, aspects (such as sun visibility and ray-tracing analysis) pose several critical considerations, especially when addressing the contextual design strategy. For example, the identification of visible sun vectors merely considers the surrounding building contexts while neglecting relevant geometric properties, such as vegetation and other site characteristics (e.g., material properties). This consequently can affect irradiation analysis during the environmental performance simulation between a proposed building and the existing contexts. Besides, the window's grid configuration lacks in representing the insolation values of building facades during the ray-tracing analysis, due to its limited consideration of geometric centroids of each surrounding window.

In order to address these gaps, the existing workflow of subtractive solar envelopes has been improved by incorporating it with the prospective application of 3D laser scanning (point cloud data). By exploiting the practical usability of the point cloud in different fields, the scope of information properties in the real contexts can be improved, and to some extent, it becomes relevant to the specific aforementioned issues. Regarding sun visibility, the 3D point cloud not only captures the most and the least sun-exposed areas through buildings and vegetation but also investigating material performances of contextual datasets through optical (reflectivity and translucency) and thermal properties (albedo and emissivity). Besides, the ray-tracing analysis between a proposed building and surrounding contexts is performed based on 3D point cloud datasets of the existing context. In other words, it substitutes the surrounding window's grid on the building facades proposed by the existing approach.

2.4. Subtractive Solar Envelopes Based on Point Cloud Data (SOLEN)

With the support of geometric and radiometric properties [53][54] stored in a 3D point cloud, the integrated computational workflow between subtractive solar envelopes and attribute information of point cloud data has been established [55][56]. It specifically integrates functional properties of position information (XYZ), color information (RGB), and reflection intensity (I). Each of these attributes caters to different potential tasks. For example, color information (RGB) can be used not only to extract and segment certain areas within the dataset based on its values [57][58], but also to translate them into new information properties [59][60]. This can include converting data attribution of RGB into HSV values to perform the measurement analysis and road maintenance [61] and extracting the semantic information of the indoor environment with automatic room labeling [62][63]. Meanwhile, reflection intensity (I) predominantly deals with surface and spectral properties of the scanned objects [64] as it constitutes the return strength values of laser pulse or backscattered echo for each recorded point [54]. Accordingly, the intensity values can be used not only to map geological layers and pavement lines [54], but also to detect natural phenomena, such as frozen and wet surfaces on roads [65], and the measurement of seasonal snow cover [66]. On the other hand, position information (XYZ) constitutes of geographic coordinate that marks each recorded point's specific location. This attribute plays a great role in synchronizing index between color and intensity values as it can attach to both attributes. Thus, complex areas of the dataset can be precisely extracted based on selected values. In general, these attributes contribute not only to extend particular performances of 3D point cloud data, such as identification of existing material properties [67], but also to extend the applicability of environmental analysis during the conceptual design stage.

Before performing the subtractive solar envelopes, the dataset correction is required to minimize erroneous levels during scanning. In this case, some aspects, such as environmental and meteorological conditions, atmospheric pollution [68][69], unit specification of the scanner, surface properties of the scanned objects, and scanning geometries [70] can principally affect metadata information of the datasets during scanning. While correcting all these variables seems impractical, due to some local constraints (i.e., manufacturers), this study specifically focuses on correcting the acquisition geometry based on the angle of incidence, which is relevant to the proposed subtractive mechanism. Having established the corrected datasets, it can be further used not only to perform the ray-tracing analysis between the 3D polyhedra and selected solar vectors, but also to calculate the material properties of existing contexts that are useful to evaluate the environmental performance of a proposed building. In parallel, insolation analysis is performed to identify the potential solar energy of the resulting solar envelopes.

3. Proposed Methods for Subtractive Shading Envelopes

This study proposes a computational framework that consists of three phases: input, simulation process, and output (see Figure 1). Within a simulation process, five sequential procedures are developed, ranging from A (input parameters) to E (form generation process of self-shading envelopes).

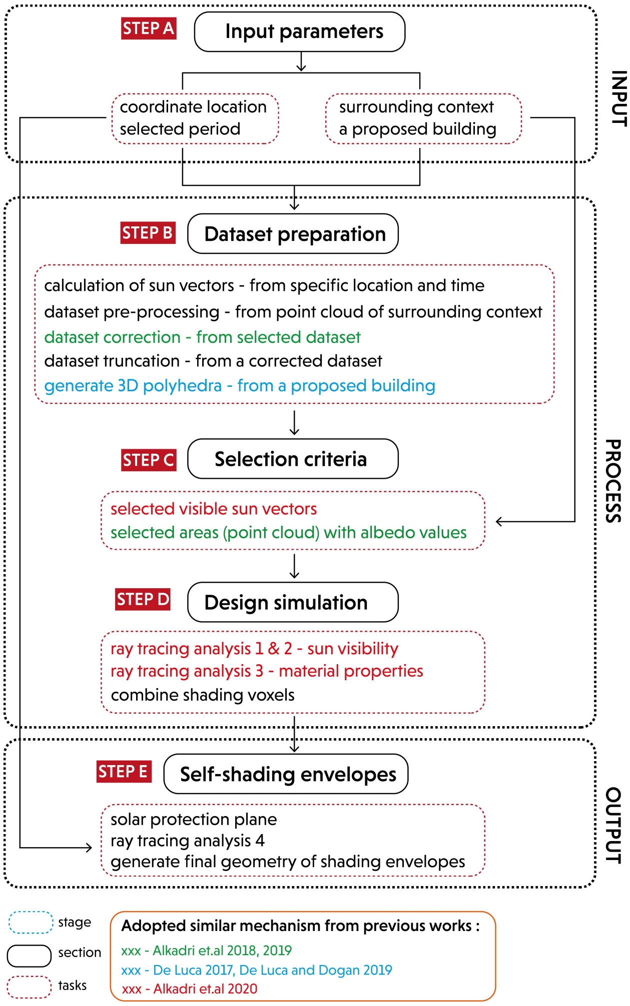

Figure 1. An overview of the proposed computational workflow.

To perform specific tasks in each predefined step, the proposed workflow was supported by several digital tools. For example, [71] was employed to collect high-resolution point cloud datasets. It was complemented with Maptek I-Site [72] to perform dataset registrations, coloring, modeling, and most importantly, to facilitate the data transfer from scanner to the workstation in any designated format. Moreover, Cloud Compare (CC) [73] was used, not only for dataset preparation, but also for dataset pre-processing, such as attribute selection, dataset formatting, scalar field features, and the normal surface calculation. In alignment with that, Matlab [74] was specifically used to assist dataset correction (i.e., optimal normal values, intensity correction, and dataset subsampling), while Rhino [75] (coupled with Grasshopper [76] for visual scripting) was employed to develop a 3D geometric model of a proposed building and to perform solar simulation analysis by using a Ladybug [77] component in Grasshopper. Furthermore, a detailed task, dataset formats, and outputs of each step are addressed below.

3.1. Stage A Input (Step A – Preparation of input parameters)

As a starting point for the computational procedures, the input section refers to step A, which contains a series of parameters that are used to construct contextual settings of the subtractive shading envelopes. Specifically, it consists of climatic properties that correspond to coordinate location (i.e., longitude and latitude position based on World Geodetic System 1984, WGS84) and selected periods (i.e., month, year, day, and hours) (see Figure 2). The longitude and latitude coordinates influence the envelope's geometrical properties on the basis of sun position and solar angle. For example, high-latitude sites are characterized by a small angle of solar altitude and smaller degrees of solar radiation. Moreover, specific periods are required to obtain the number of critical hours of natural illumination that affects a proposed building and surrounding contexts.

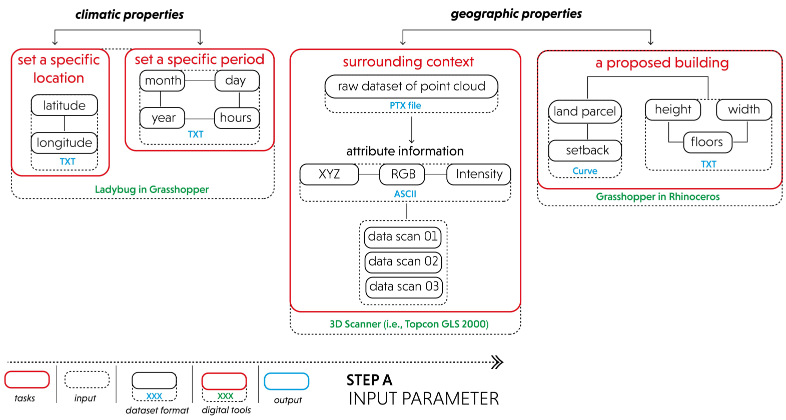

Figure 2. Preparation of input parameters.

On the other hand, geographic properties include surrounding contexts (i.e., existing buildings and vegetation) and a geometric model of the proposed building. In this regard, the surrounding context contains a 3D point cloud data of the existing environment. As a raw dataset, its format properties often rely on the type of 3D scanner, but as long as the required attribute information (i.e., XYZ, RGB, and reflection intensity) is legible, any raw dataset formats are acceptable (i.e., PTX file). Meanwhile, several parameters, such as height, width, floors, setback, and building function, must be established to generate an initial 3D envelope for a proposed building. These inputs are then executed into the following Step B (dataset preparation) based on corresponding parameters and tasks.

3.2. Stage B Simulation Process

This section focuses on translating the raw datasets into a simulation model by examining three main steps (i.e., dataset preparation, selection criteria, and form generation process of shading envelopes). Each step serves specific actions that are performed sequentially based on specific computational tasks. As illustrated in Figure 1, this section adopts several workflows that are partially implemented from previous works. For example, pre-processing point cloud datasets and the calculation of material properties (i.e., albedo values) are indicated with a green text [67]. These works focused on developing a material database of existing contexts and solar radiation analysis based on a small sample of point cloud data. Next, 3D polyhedra and sun visibility analysis are illustrated in the blue text [49][50]. These works primarily investigated a voxel-based generative design of subtractive solar envelopes based on 3D and parametric modelling. Last, the ray-tracing analysis between a proposed building and point cloud data of surrounding contexts is illustrated in the red text [56]. This work refers to a form generation of subtractive solar envelopes that consider surface properties of existing contexts based on geometric and radiometric information of point cloud data. While these previous works address different objectives, some features are still relevant for supporting an integrated design concept and computational workflow for establishing the subtractive shading envelopes.

To illustrate specific tasks in this stage, a detailed discussion of each proposed step is presented below.

3.2.1 Step B – Dataset preparation

This step aims to prepare all the necessary datasets to be readily used in the simulation model. After establishing the input from climatic and geographic properties, five tasks are required to perform. Two of these tasks (i.e., sun vectors calculation and the initial envelopes generation) can be run in parallel while the other three tasks (i.e., pre-processing datasets, dataset correction, and subsampling dataset) can be executed sequentially (see Figure 3).

Task 1, sun vectors refer to the number of sunlight hours that must be preserved on surrounding facades during the required period. As compared with cut-off times, which refer to a fixed period, sun access duration can be selected from a range of available hours for a specific façade on a specific day or for each day during a specific period. In doing so, sun visibility plays a crucial role when determining the relevant sun vectors.

Task 2, the initial envelope of a proposed building, is generated based on the predefined criteria. In this case, the functional program of a proposed building is projected as a public library as well as communal space for the local community. To support the main activities, some spaces are established, such as a reading room, meeting room, toilet, and exhibition areas. Accordingly, the building needs to be accessible, and its indoor environment should be thermally comfortable for supporting the daily activities.

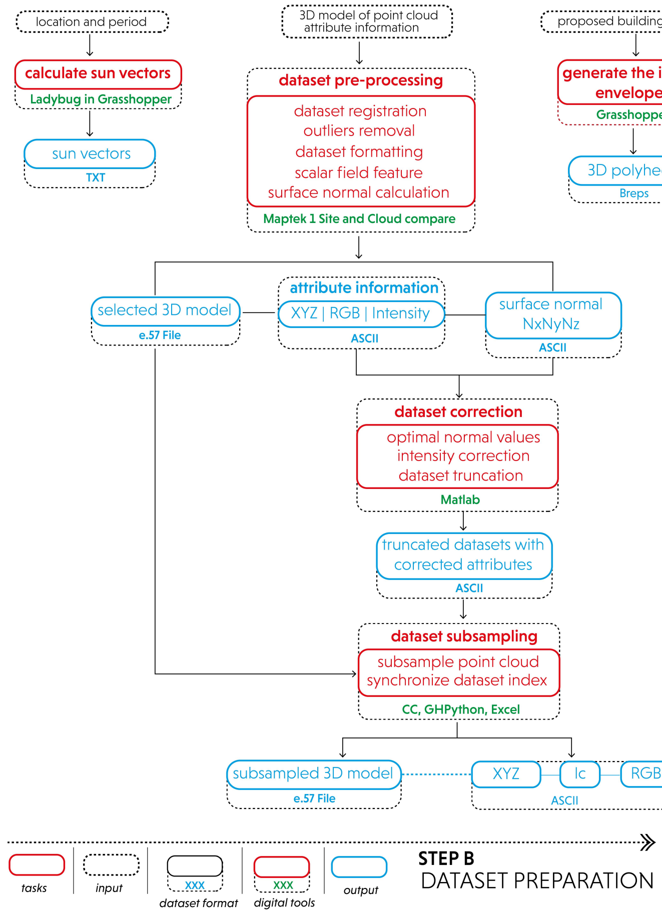

Figure 3. Detailed procedures for the dataset preparation.

Task 3, the pre-processing tasks start with the dataset registration. This process aims to locate recorded datasets into a standard coordinate system based on the reflector position and GPS orientation. Afterward, the outlier (unnecessary cloud of points) removal is performed not only to clean the boundary of selected datasets but also to filter noises created during scanning. The dataset formatting also plays an important role in compensating for interoperability issues during the simulation process. In this case, the initial format of 3D raw point clouds (i.e., PTX) and its metadata are converted to E57 and ASCII files, respectively, in order to be accessible for various digital processing tools. In addition to this, the scalar field of the dataset is activated to identify the attached values' scale in each attribute. Last, surface normals (NxNyNz) of the dataset are calculated to find the appropriate normal values of each projected point during scanning. As normal values of the raw point cloud are excluded in the typical attribute properties, various angles of incidence, ranging from the sample of 10° to 90°, are firstly computed to each data scan. This is done by using the Hough Normal plugin [78] in CC due to the original form of unstructured raw point cloud data. In this regard, each point within each data scan has different preliminary normal values. Ultimately, task 3 results in several outputs such as a 3D model of selected datasets, attribute information of point cloud data with raw intensity values, and normal surface of each data scan at various incidence angles.

Task 4, the dataset correction, is performed to compensate for the scattering condition of unstructured point clouds during scanning, specifically for amending radiometric properties of the dataset. It is worth noting that this procedure can only be applied on a single scan due to the potentiality of mixing a reference point of the scanner and intensity values on the merge datasets [54]. The correction step starts with finding the average distribution of optimal projection points from the preliminary normal values. This allows for achieving a reliable surface normal on each applied angle in the data scan. To do so, the following equation [79] is applied with an assumption that the original position of a 3D scanner located at (0,0,0).

$$i = \cos^{-1}\left(\frac{\overline{dn}.\overline{dl}}{|\overline{dn}||\overline{dl}|}\right) \quad (1)$$

where i = initial incidence angle
$\overline{dn}$ = direction of the surface normal
$\overline{dl}$ = direction of the laser pulse

After configuring the point distribution from a various range of cosinus products, an evaluation is conducted to the standard deviation of each registered cosine value within the dataset. It aims to identify the pattern of point density to reduce scattered and coarse point clouds through the dataset truncation. Afterward, the truncated datasets can be used for the intensity correction. In this regard, the angle of incidence becomes a relevant factor for correcting the dataset's acquisition geometry, given that instrumental effects highly affect the raw intensity value of TLS datasets. This procedure is executed based on the following equation [55].

$$I_c = I_{raw} \cdot \frac{1}{\cos\ \alpha} \quad (2)$$

where I_c = corrected intensity
I_{raw} = original intensity
α = angle of incidence

Task 5, the subsampling dataset, is performed in CC to reduce the density of points during the simulation. However, this procedure creates interoperability issues when the resulting dataset is matched and visualized to the initial 3D model in Rhino. Specifically, the 3D model cannot directly recognize the input of subsampled datasets due to different units and scales of the attribute information. Therefore, synchronizing the initial index between the two datasets allows the identification of metadata information in the geometric 3D model. This further permits the extraction of certain areas in the 3D dataset based on selected attributes values.

3.2.2 Step C – Selection criteria

After preparing the corrected datasets from climatic and geographic properties, this study sets two environmental performance criteria that support the geometric generation: sun visibility and material properties (see Figure 4). Sun visibility plays a crucial role in filtering the sun vectors that have direct access to the dataset of surrounding contexts. To do so, sun vectors generated from the indicated period are multiplied with normal vectors extracted from subsampled datasets. The resulting normal irradiance values are then evaluated on the basis of the projected angle. In this case, irradiance values with equal and larger than 90° are eliminated as they consist of zero and negative cosine values. Accordingly, these values are then excluded within the list of visible sun vectors because the surface of the datasets does not properly absorb their solar energy. Afterward, the resulting values can be used to select the corresponding points within the dataset.

On the other hand, material aspects are used to measure the performance behavior of the existing site's surface properties. This allows architects to identify susceptible areas that may affect the geometrical performance of the proposed design. This study specifically computes albedo values to detect the absorbance percentage of solar energy on surrounding contexts by considering the RGB color and corrected intensity (Ic) of contextual datasets. A detailed procedure regarding the calculation of albedo values can be found in our previous research [67]. Furthermore, the resulting albedo values are filtered based on the threshold below 0.3. Although this setting indicates the low albedo, it can be used not only to identify areas that contain a high level of heat absorbance but also to analyze and mitigate microclimatic impacts of the surrounding areas especially related to thermal issues and urban heat island (UHI) effect. In order to avoid that, these areas need to be blocked from direct sun exposures by excluding the indicated surfaces with high albedo values. Afterward, the resulting indexes of low albedo values (below 0.3) are synchronized not only with selected normal vectors from the sun visibility to register the corresponding surface normal of the dataset but also with XYZ attributes to select the matching points within the dataset.

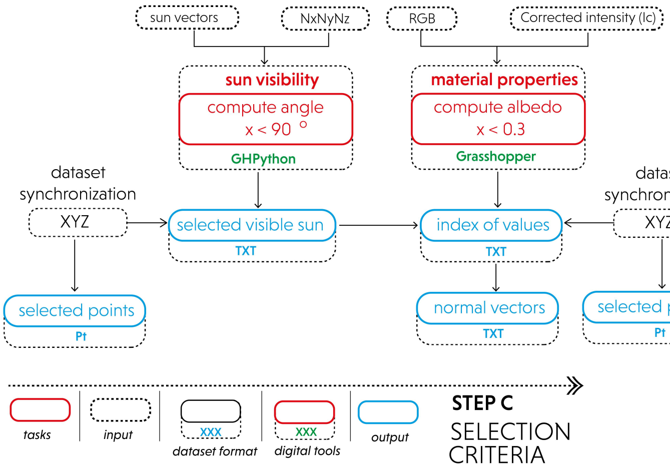

Figure 4. Selection procedures based on the criteria of sun visibility and material properties.

3.2.2 Step D – Form generation process of shading envelopes

After establishing all the required parameters from the selection criteria, this step focuses on developing the simulation workflow (see Figure 5). It starts with the first ray-tracing analysis that requires input from visible sun vectors, selected corresponding points from sun visibility, and 3D polyhedra of a proposed building. This procedure principally applies a Boolean expression to assign true or false conditions on selected voxels within the 3D polyhedral array. The ray-tracing analysis-01 generates intersecting rays that are then evaluated based on the predefined criteria of direct sun access. In this case, voxels that are not blocking sun access to the proposed buildings or are categorized as an unsuccessful intersection with the 3D polyhedra will be considered part of the shading voxels (refer to voxels-02 in Figure 5). This workflow can also be called as a reverse solar envelope. Meanwhile, voxels that receive sun access will be forwarded to a later step in the second ray-tracing analysis (refer to voxels-01 in Figure 5).

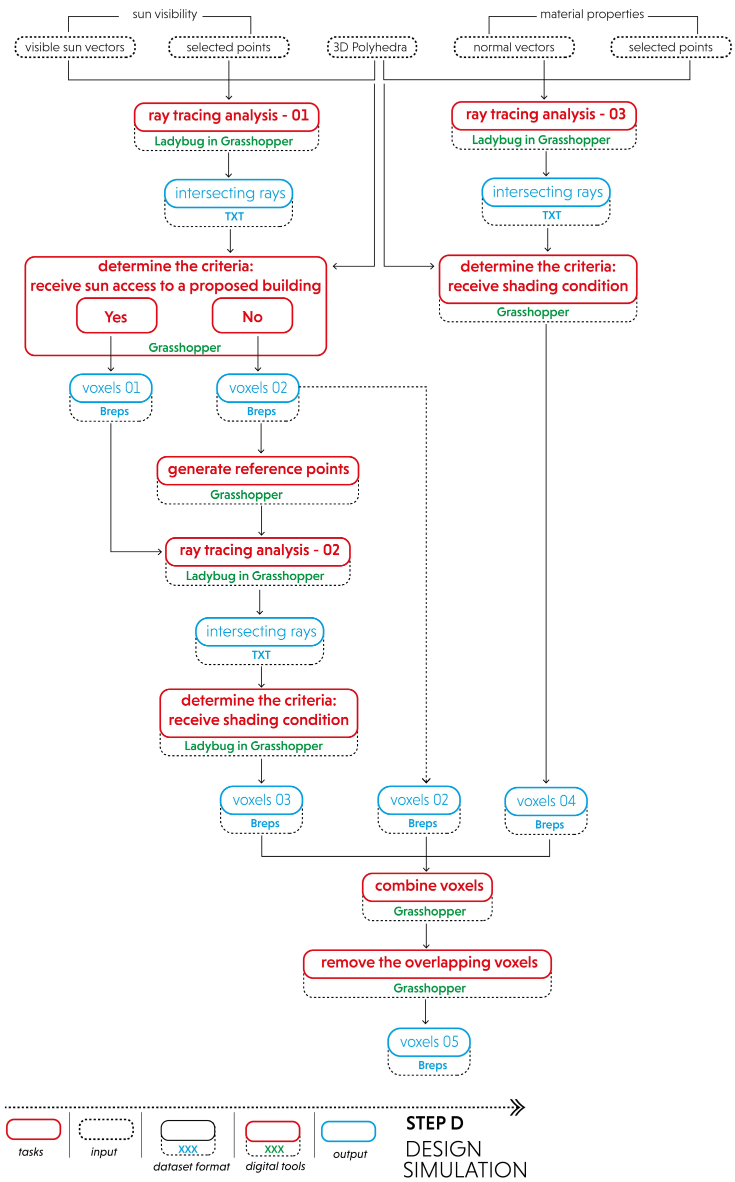

Figure 5. Detailed procedures for the design simulation.

Furthermore, reference points are generated from the voxels-02 to be used in the simulation of ray-tracing analysis-02. As a follow-up to the previous procedure, the ray-tracing analysis-02 aims to maximize the geometric generation of shading voxels. In doing so, by changing the basis projection of initial reference points originated from surrounding buildings to the voxels-02 may compensate for geometric obstruction of polyhedra at a certain projection angle in the ray-tracing analysis-01. Instead of applying this procedure to the original 3D polyhedra, it is used to re-evaluate voxels-01 based on reference points of voxels-02 so as to identify additional voxels (refer to voxels-03) that fulfill the criteria of receiving shading condition. As for the input for material properties, a similar procedure of ray-tracing analysis is also performed by considering the lowest albedo values (ranging from 0 to 0.3) applied to surround contexts. These results in voxels-04 so that in total, three groups of voxels (i.e., voxels-02, voxels-03, and voxels-04) are generated to shade surrounding buildings. These voxels are then combined into one group, voxels-05. To ensure that a shading condition also applies on a proposed building, the self-shading workflow is performed in the following stage.

3.3 Stage C Output (Step E – Form generation process of self-shading envelopes)

As a last stage of the computational workflow, the output contains final tasks to generate a geometric configuration of self-shading envelopes (see Figure 6). The first task begins with selecting the upper part of the stacking voxels. This upper part acts as a roof or shelter to guarantee a shading condition for all properties under its envelope within a predefined period. Afterward, a solar protection plane can be applied on the bottom surfaces of the upper part of the voxels. It aims to establish reference points that are used as the basis for ray projections. Furthermore, the ray-tracing analysis-04 is performed by considering inputs from reference points of the upper voxels, the remaining stacking voxels (i.e., bottom part), and initial sun vectors calculated for the analysis period under consideration. This simulation will evaluate the remaining voxels by maintaining the one that receives a shading condition while removing the unshaded voxels. The resulting voxels (refer to voxels-06) are then combined with the upper voxels to establish the geometric envelope for each data scan (refer to voxels-07 and voxels-08). After identifying self-shading voxels for each data scan, the final step is to combine all these voxels into a final geometric envelope that represents a final configuration of envelopes (refers to voxels-09).

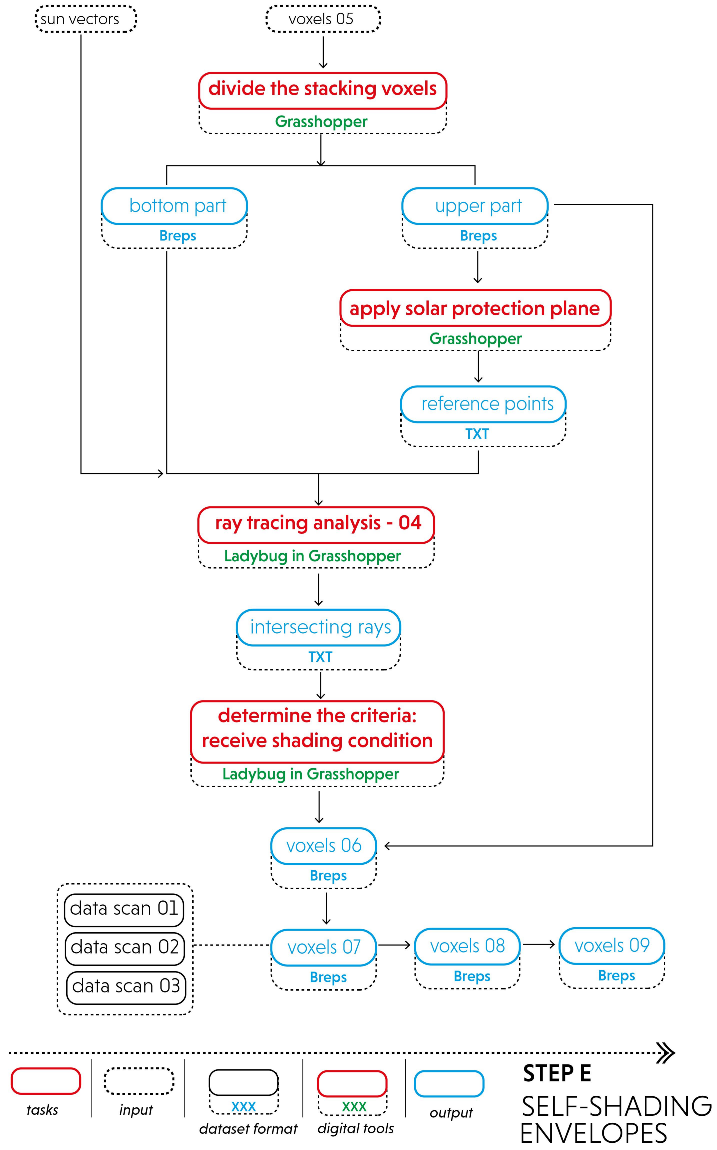

Figure 6. Detailed procedures for generating the final output of self-shading envelopes.

References

1. Shih, N.-J.; Wu, M.-C. A 3D Point-Cloud-Based Verification of as-Built Construction Progress. In Proceedings of the CAAD Futures 2005 Conference, Vienna, Austria, 20–22 June 2005.
2. Alsadik, B.; Gerke, M.; Vosselman, G. Visibility analysis of point cloud in close range photogrammetry. ISPRS Ann. Photogr. Remote Sens. Spat. Inf. Sci. 2014, 2, 9–16.
3. Andriasyan, M.; Moyano, J.J.; Julián, J.E.N.; García, D.A. From Point Cloud Data to Building Information Modelling: An Automatic Parametric Workflow for Heritage. Remote Sens. 2020, 12, 1094.
4. Shanoer, M.M.; Abed, F.M. Evaluate 3D laser point clouds registration for cultural heritage documentation. Egypt. J. Remote Sens. Space Sci. 2018, 21, 295–304.
5. Remondino, F. Heritage Recording and 3D Modeling with Photogrammetry and 3D Scanning. Remote Sens. 2011, 3, 1104–1138.
6. Núñez-Andrés, M.A.; Buill, F.; Costa-Jover, A.; Puche, J.M. Structural assessment of the Roman wall and vaults of the cloister of Tarragona Cathedral. J. Build. Eng. 2017, 13, 77–86.
7. Bornaz, L.; Lingua, A.; Rinaudo, F. Engineering and Enviroonmental Applications of Laser Scanner Techniques. In Proceedings of the ISPRS Commission III Symposium Photogrammetric Computer Vision, Graz, Austria, 9–13 September 2002.
8. Kassner, R.; Koppe, W.; Schüttenberg, T.; Bareth, G. Analysis of the Solar Potential of Roofs By Using Official Lidar Data. In Proceedings of the ISPRS Congress, Beijing, China, 3–11 July 2008.

9. Carneiro, C.; Morello, E.; Desthieux, G. Assessment of Solar Irradiance on the Urban Fabric for the Production of Renewable Energy using LIDAR Data and Image Processing Techniques. In Proceedings of the Advances in GIScience, Hannover, Germany, 2–5 June 2009.
10. Desthieux, G.; Carneiro, C.; Camponovo, R.; Ineichen, P.; Morello, E.; Boulmier, A.; Abdennadher, N.; Dervey, S.; Ellert, C. Solar Energy Potential Assessment on Rooftops and Facades in Large Built Environments Based on LiDAR Data, Image Processing, and Cloud Computing. Methodological Background, Application, and Validation in Geneva (Solar Cadaster). Front. Built Environ. 2018, 4, 1–22.
11. Staneva, N.N. Approaches for generating 3D solid models in AutoCAD and solid works. J. Eng. 2008, 3, 28–31.
12. Shapiro, V. Spatial Automation Laboratoty. In Solid Modeling; University of Wisconsin: Madison, WI, USA, 2001.
13. Otepka, J.; Ghuffar, S.; Waldhauser, C.; Hochreiter, R.; Pfeifer, N. Georeferenced Point Clouds: A Survey of Features and Point Cloud Management. ISPRS Int. J. Geoinf. 2013, 2, 1038–1065.
14. Richter, R.; Döllner, J. Concepts and techniques for integration, analysis and visualization of massive 3D point clouds. Comput. Environ. Urban Syst. 2014, 45, 114–124.
15. Arayici, Y. Towards building information modelling for existing structures. Struct. Surv. 2008, 26, 210–222.
16. Alkadri, M.F.; Turrin, M.; Sariyildiz, S. The use and potential applications of point clouds in simulation of solar radiation for solar access in urban contexts. Adv. Comput. Des. 2018, 3, 319–338.
17. Knowles, R.L. Energy and Form: An Ecological Approach to Urban Growth, Cambridge; The MIT Press: Cambridge, MA, USA, 1974.
18. Knowles, R.L. Sun, Rhytm and Form, Massachusetts; The MIT Press: Cambridge, MA, USA, 1981.
19. Alkadri, M.F.; De Luca, F.; Turrin, M.; Sariyildiz, S. Understanding Computational Methods for Solar Envelopes Based on Design Parameters, Tools, and Case Studies: A Review. Energies 2020, 13, 3302.
20. GlobalABC, IEA and UN. 2019 Global Status Report for Buildings and Construction: Towards a Zero-Emission, Efficient and Resilient Buildings and Construction Sector; IEA and United Nations Environment Programme: Madrin, Spain, 2019.
21. Chandel, S.; Sharma, V.; Marwah, B.M. Review of energy efficient features in vernacular architecture for improving indoor thermal comfort conditions. Renew. Sustain. Energy Rev. 2016, 65, 459–477.
22. Ehzan, M.; Farshchi, M.A.; Ford, A. Vernacular Architecture And Energy Use In Buildings: A Comparative Study. IJAMCE 2015, 2, 35–42.
23. Lepore, M. The right to the sun in the urban design. Vitr. Int. J. Arch. Technol. Sustain. 2017, 2, 24–43.
24. Mazzone, D. The Dark Side of a Model Community: The Ghetto of el-Lahun. J. Anc. Egypt. Archit. 2017, 2, 19–54.
25. Butti, K.; Perlin, J. A Golden Threat 2500 Years of Solar Architecture and Technology; Van Nostrand Reinhold Company: New York, NY, USA, 1980.
26. Giacomo, L. The Architecture of A. Palladio in Four Books; John sWatts: London, UK, 1715.
27. Curreli, S.; Coch, H. Solar access in the compact city: A study case in Barcelona. In Proceedings of the 3rd International Conference PALENC 2010 Passive & Low Energy Cooling for the Built Environment, Rhodes Island, Greece, 29 September-1 October 2010.
28. Wang, X.; Wei, Z.-S.; Pang, X. Solar design in the application of the city planning. In Proceedings of the International Conference on Low-Carbon Transportation and Logistics, and Green Buildings, Beijing, China, 12–13 October 2012.
29. Sarkar, A. Low energy urban block: Morphology and urban guidelines. In Proceedings of the 45th ISOCARP Congress, Porto, Portugal, 18–22 October 2009.
30. Alkadri, M.F.; Turrin, M.; Sariyildiz, S. The use and potential applications of point clouds in simulation of solar radiation for solar access in urban contexts. Advances Comput. Des. 2018, 3, 319–338.
31. Littlefair, P.J.; Santamouris, M.; Alvarez, S.; Dupagne, A.; Hall, D. Environmental Site Layout Planning: Solar Access, Microclimate and Passive Cooling in Urban Areas; Construction Research Communications Ltd.: London, UK, 2000.
32. Dekay, M.; Brown, G.Z. Sun, Wind & Light: Architectural Design Strategies, 3th ed.; John Wiley & Sons: Hoboken, NJ, USA, 2014.
33. Emmanuel, R. A Hypothetical ‘Shadow Umbrella’ for Thermal Comfort Enhancement in the Equatorial Urban Outdoors. Arch. Sci. Rev. 1993, 36, 173–184.
34. DeKay, R.M. Climatic urban design: Configuring the urban fabric to support daylighting, passive cooling, and solar heating. Sustain. City VII 2012, 1, 619–630.

35. Dinić, M.; Mitković, P. Planning regulations in the USA and their implications on urban design in the central city zone. Facta Univ. Arch. Civ. Eng. 2011, 9, 289–299.

36. Szokolay, S.V. Introduction to Architectural Science: The Basis of Sustainable Design; Architectural Press: Oxford, UK, 2004.

37. Capeluto, I.G. Energy performance of the self-shading building envelope. Energy Build. 2003, 35, 327–336.

38. Yezioro, A.; Shaviv, E. Shading: A design tool for analyzing mutual shading between buildings. Sol. Energy 1994, 52, 27–37.

39. Marsh, A. Computer-Optimised Shading Design. In Proceedings of the Eight International IBPSA Conference,Eindhoven, The Netheerlands, 11-14 August 2003.

40. Stevanović, S.; Stevanović, D.; Dehmer, M. On optimal and near-optimal shapes of external shading of windows in apartment buildings. PLoS ONE 2019, 14, e0212710.

41. Kabre, C. Winshade: A computer design tool for solar control. Build. Environ. 1998, 34, 263–274.

42. Etzion, Y. An improved solar shading design tool. Build. Environ. 1992, 27, 297–303.

43. Sargent, J.; Niemasz, J.; Reinhart, C.F. In Proceedings of the SHADERADE: Combining Rhinoceros and Energyplus for the Design of Static Exterior Shading Devices, Sydney, Australia, 14–16 November 2011.

44. Kaftan, E.; Marsh, A. Integrating the cellular method for shading design with a thermal simulation. In Proceedings of the International Conference “Passive and Low Energy Cooling for the Built Environment”, Santorini, Greek, 19–1 May 2005.

45. Leidi, M.; Schlüter, A. Exploring urban space—Volumetric site analysis for conceptual design in the urban context. Internatl. J. Archit. Comput. 2013, 11, 157–182.

46. Leidi, M.; Schlüter, A. Volumetric insolation analysis. In Proceedings of the CleanTech for Sustainable Buildings—From Nano to Urban Scale (CISBAT 2011), Lausanne, Switzerland, 14–16 September 2011.

47. Ozel, F. SolarPierce: A Solar Path-Based Generative System. In Proceedings of the Computation and Performance—Proceedings of the 31st eCAADe Conference, Delft, Netherlands, 18–20 September 2013.

48. Da Veiga, J.; La Roche, P. A Computer Solar Analysis Tool for the Design and Manufacturing of Complex Architectural Envelopes: EvSurf. In Proceedings of the SIGraDi 2002, 6th Iberoamerican Congress of Digital Graphics, Caracas, Venezuela, 27–29 November 2002.

49. Littlefair, P. Passive solar urban design: Ensuring the penetration of solar energy into the city. Renew. Sustain. Energy Rev. 1998, 2, 303–326.

50. De Luca, F. Solar form finding. In Proceedings of the 37th Annual Conference of the Association for Computer Aided Design in Architecture: Disciplines and Disruption, ACADIA, Cambridge, UK, 2–4 November 2017.

51. De Luca, F.; Dogan, T. A novel solar envelope method based on solar ordinances for urban planning. Build. Simul. 2019, 12, 817–834.

52. De Luca, F.; Voll, H. Computational method for variable objectives and context-aware solar envelopes generation. In Proceedings of the 8th Annual Symposium on Simulation for Architecture and Urban Design, SimAUD, Toronto, ON, Canada, 22–24 May 2017.

53. Darmon, I. Voxel computational morphogenesis in urban context: Proposition and analysis of rules-based generative algorithms considering solar access. In Proceedings of the Advanced Building Skins, Bern, Switzerland, 28–29 October 2019.

54. Kaasalainen, S.; Krooks, A.; Kukko, A.; Kaartinen, H. Radiometric Calibration of Terrestrial Laser Scanners with External Reference Targets. Remote Sens. 2009, 1, 144–158.

55. Kashani, A.G.; Olsen, M.J.; Parrish, C.E.; Wilson, N. A Review of LIDAR Radiometric Processing: From Ad Hoc Intensity Correction to Rigorous Radiometric Calibration. Sensors 2015, 15, doi:10.3390/s151128099.

56. Alkadri, M.F.; De Luca, F.; Turrin, M.; Sariyildiz, S.; Making use of point cloud for generating subtractive solar envelopes. In Proceedings of the eCAADe SIGraDi 2019: Architecture in the Age of the 4th Industrial Revolution, Porto, Portugal, 7 September 2020.

57. Alkadri, M.; De Luca, F.; Turrin, M.; Sariyildiz, I.S. An integrated approach to subtractive solar envelopes based on attribute information from point cloud data. Renew. Sustain. Energy Rev. 2020, 123, 109742.

58. Fujita, Y.; Hoshino, Y.; Ogata, S.; Kobayashi, I. Attribute Assignment to Point Cloud Data and Its Usage. Glob. J. Comp. Sci. Technol. 2015, 15, 2.

59. Zhan, Q.; Yu, L.; Liang, Y. A point cloud segmentation method based on vector estimation and color clustering. In Proceedings of the 2nd International Conference on Information Science and Engineering (ICISE), Hangzhou, China, 4–6 December 2010.

60. Kobayashi, I.; Fujita, Y.; Sugihara, H.; Yamamoto, K. Attribute Analysis of Point Cloud Data with Color Information. J. Jpn. Soc. Civ. Eng. Ser. F3 Civil Eng. Inform. 2011, 67, doi:10.2208/jscejcei.67.i_95.

61. Aijazi, A.K.; Checchin, P.; Trassoudaine, L. Segmentation Based Classification of 3D Urban Point Clouds: A Super-Voxel Based Approach with Evaluation. Remote Sens. 2013, 5, 1624–1650.

62. Fujita, Y.; Kobayashi, I.; Chanseawrassamee, W.; Hoshino, Y. Application of Attributed Road Surface Point Cloud Data in Road Maintenance. J. Jpn. Soc. Civ. Eng. Ser. F3 Civil Eng. Inform. 2014, 70, doi:10.2208/jscejcei.70.i_185.

63. Tamke, M.; Blümel, I.; Ochman, S.; Vock R.; Wessel, R. From point clouds to definitions of architectural space: Potentials of automated extraction of semantic information frompoint clouds for the building profession. In Proceedings of the eCAADe, Newcastle upon Tyne, UK, 10 September 2014.

64. Turner, E.; Cheng, P.; Zakhor, A. Fast, Automated, Scalable Generation of Textured 3D Models of Indoor Environments. IEEE J. Sel. Top. Signal Process. 2014, 9, 409–421.

65. Tan, K.; Cheng, X. Correction of Incidence Angle and Distance Effects on TLS Intensity Data Based on Reference Targets. Remote Sens. 2016, 8, 251.

66. Shin, J.-I.; Park, H.; Kim, T. Characteristics of Laser Backscattering Intensity to Detect Frozen and Wet Surfaces on Roads. J. Sens. 2019, 2019, 1–9.

67. Kaasalainen, S.; Kaartinen, H.; Kukko, A. Snow cover change detection with laser scanning range and brightness measurements. EARSeL eProc. 2008, 7, 133–141.

68. Alkadri, M.F.; Turrin, M.; Sariyildiz, S. A computational workflow to analyse material properties and solar radiation of existing contexts from attribute information of point cloud data. Build. Envir. 2019, 155, 268–282.

69. Suchocki, C.; Błaszczak-Bąk, W. Down-Sampling of Point Clouds for the Technical Diagnostics of Buildings and Structures. Geoscience 2019, 9, 70.

70. Armesto, J.; Riveiro, B.; González-Aguilera, D.; Rivas-Brea, M.T. Terrestrial laser scanning intensity data applied to damage detection for historical buildings. J. Archaeol. Sci. 2010, 37, 3037–3047.

71. Soudarissanane, S. The Geometry of Terrestrial Laser Scanning; Identification of Errors, Modeling and Mitigation of Scanning Geometry. Ph.D. Thesis, Faculty of Civil Engineering and Geosciences, TU Delft, Delft, The Netherlands, January 2016.

72. TOPCON. GLS-2000 Series: Multi Functional 3D Laser Scanner. Available online: https://www.topconpositioning.com/sites/default/files/product_files/gls-2000series_broch_7010-2152_reve_team_en_us_lores.pdf (accessed on 6 January 2020).

73. Maptek. Maptek I-Site Studio; Maptek: Denver, USA, 2015.

74. Compare, C. Cloud Compare: 3D point cloud and mesh processing software, open source project. 2019. Available online: http://www.cloudcompare.org/ (accessed on 1 April 2020).

75. Matlab. MathWorks. 2020. Available online: https://nl.mathworks.com/products/matlab.html?s_tid=hp_ff_p_matlab (accessed on 2 April 2020).

76. Rhinoceros. Rhinoceros: design, model, present, realize, analyse...2020. Available online: https://www.rhino3d.com/ (accessed on 4 April 2020).

77. Davidson, Scoot. Grasshopper: Algorithmic modelling for rhino. 2020. Available online: https://www.grasshopper3d.com/ (accessed on 4 April 2020).

78. Ladybug. Ladybug tools. 2020. Available online: https://www.ladybug.tools/ (accessed on 5 April 2020).

79. Boulch, A.; Marlet, R. Deep Learning for Robust Normal Estimation in Unstructured Point Clouds. In Proceedings of the Eurographics Symposium on Geometry Processing, Berlin, Germany, 20–24 June 2016.